nature materials

ARTICLES

PUBLISHED ONLINE: 23 OCTOBER 2011 | DOI: 10.1038/NMAT3146

Electrochemical activation and inhibition of neuromuscular systems through modulation of ion concentrations with ion-selective membranes

Yong-Ak Song[1,2], Rohat Melik[1,2], Amr N. Rabie[3,4], Ahmed M. S. Ibrahim[3], David Moses[5], Ara Tan[6], Jongyoon Han[1,2]* and Samuel J. Lin[3]*

Conventional functional electrical stimulation aims to restore functional motor activity of patients with disabilities resulting from spinal cord injury or neurological disorders. However, intervention with functional electrical stimulation in neurological diseases lacks an effective implantable method that suppresses unwanted nerve signals. We have developed an electrochemical method to activate and inhibit a nerve by electrically modulating ion concentrations *in situ* along the nerve. Using ion-selective membranes to achieve different excitability states of the nerve, we observe either a reduction of the electrical threshold for stimulation by up to approximately 40%, or voluntary, reversible inhibition of nerve signal propagation. This low-threshold electrochemical stimulation method is applicable in current implantable neuroprosthetic devices, whereas the on-demand nerve-blocking mechanism could offer effective clinical intervention in disease states caused by uncontrolled nerve activation, such as epilepsy and chronic pain syndromes.

The initiation and conduction of nerve impulses are based on the electrochemical processes localized in the surface structure of nerve cells and their axons[1], which have been quantitatively described by the Hodgkin–Huxley model[2]. Roles of various ionic species (K^+, Na^+ and Ca^{2+}) in the propagation of action potentials have been well characterized, both theoretically and experimentally. Extracellular potassium concentration largely determines the resting potential of axons, whereas the sodium concentration gradient is mainly responsible for the generation of action potentials. The role of calcium ions in nerve stimulation is known to be the gating of potassium ion channels[3]. Local, temporary modulation of these ion concentrations would enable new modes of control and manipulation of the nervous system, but such methods have never been realized in the context of prosthetic devices and *in vivo* situations. On the basis of the role of potassium, sodium and calcium[4,5] ions in neural processes, we developed an electrochemical method by using ion-selective membranes (ISMs) to modulate the ion concentration *in situ* to change the nerve excitability locally at the site of electrical stimulation for more efficient stimulation, or along the nerve fibre for more efficient on-demand suppression of nerve signal propagation. The K^+, Na^+ and Ca^{2+} ion concentration modulation was achieved by running small direct currents (10 to 100 times smaller than functional electrical stimulation thresholds) through either K^+, Na^+ or Ca^{2+} ISMs, therefore inducing local, dynamic and selective depletion of target ions immediately juxtaposed to the nerve. Our approach is based on a microfabricated ISM and eliminates the requirement of a chemical reservoir in the implant with traditional chemical stimulation methods[6,7], significantly simplifying system design and operation. These ions are naturally present in the interstitial fluid near the nervous system *in vivo*.

Enhancing neuromuscular stimulation with Ca^{2+} ISMs

For *in vitro* experiments, we placed a sciatic nerve (with perineurium and epineurium preserved) on a microfabricated planar gold electrode array and stimulated the nerve electrically (Fig. 1). Details of the fabrication of ion-selective microelectrodes and preparation of frogs are given in the Methods section. First, we applied an ion-depletion current i_d across the ISM between two diametrically opposite electrodes in the centre, as shown schematically in Fig. 2a. We limited the ion depletion current i_d to $\leq 1\,\mu A$, which was well below nominal current thresholds for electrical stimulation. The planar microelectrode covered with the ISM acted as a cathode and the opposite electrode as an anode to deplete the positively charged Ca^{2+} ions. After depleting the ions at a given current i_d for a duration t_d, we applied an electrical stimulus current i_s between the two outer stimulating electrodes and the centre contact electrode (covered with the Ca^{2+} ISM) while i_d across the ISM was off (Fig. 2b). Stimulation threshold currents, as well as the resulting muscle contraction force originating from the stimulation, were simultaneously measured and compared between conditions (see Methods section).

In all tests, we first measured the electrical current stimulation threshold using bare gold electrodes without ion depletion or modulation. Although there was a variation between different animal preparations, we used a standard pulse train between

[1]Department of Electrical Engineering and Computer Sciences, Massachusetts Institute of Technology, Cambridge, Massachusetts 02139, USA, [2]Department of Biological Engineering, Massachusetts Institute of Technology, Cambridge, Massachusetts 02139, USA, [3]Divisions of Plastic Surgery and Otolaryngology, Beth Israel Deaconess Medical Center, and Harvard Medical School, Boston, Massachusetts 02215, USA, [4]Department of Otolaryngology, Ain Shams University, Cairo 11566, Egypt, [5]Department of Bioengineering, Rice University, Houston, Texas 77005, USA, [6]Department of Chemical Engineering, University of Minnesota, Twin Cities, Minnesota 55455, USA. *e-mail: jyhan@mit.edu; sjlin@bidmc.harvard.edu.

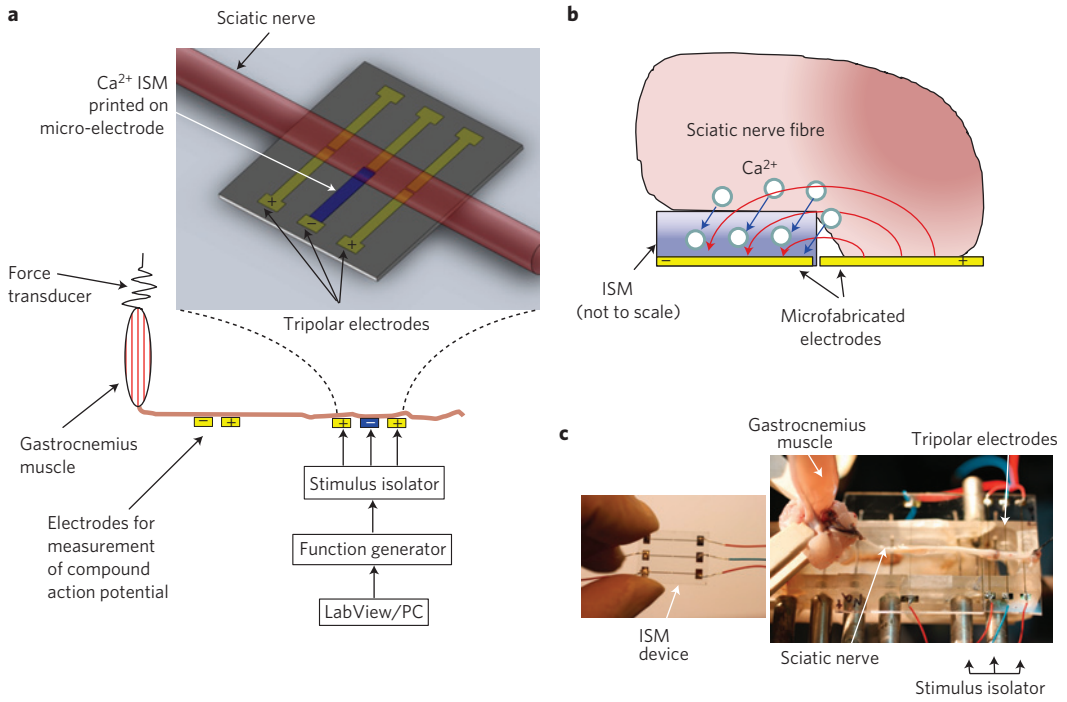

Figure 1 | Principle and experimental set-up of functional electrochemical stimulation with *in situ* ion concentration modulation through ISMs. **a**, Schematic diagram of the experimental set-up with a planar tripolar ISM electrode array for electrochemical stimulation of frog sciatic nerves with data acquisition of muscle contractile forces and compound action potentials. **b**, Schematic view of a Ca^{2+} ISM surface-printed on top of a planar microelectrode. When applying direct current across two adjacent planar microelectrodes, the positively charged Ca^{2+} ions in the nerve become depleted locally near the membrane, resulting in higher excitability for electrical stimulation. Using a microfabrication technique, the distance between the two electrodes as well as the thickness of the surface-printed ISM can be precisely controlled. **c**, Experimental set-up for stimulation of frog sciatic nerve with a Ca^{2+} ISM device.

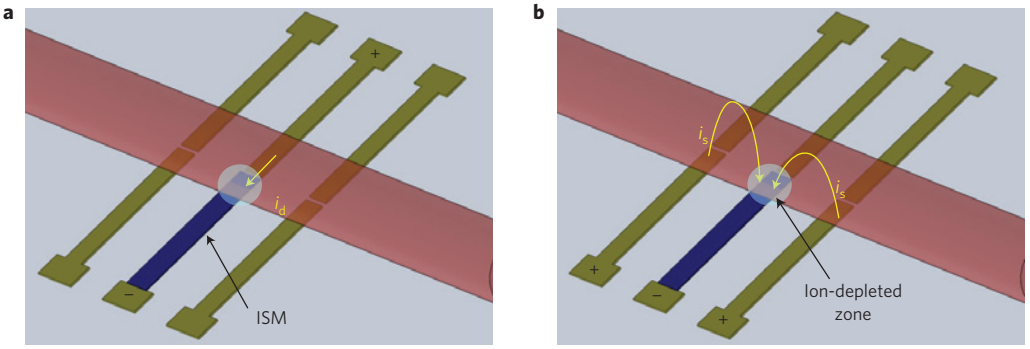

Figure 2 | Operation modes of electrochemical stimulation with modulation of the local ion concentration adjacent to a nerve. a, In the ion-depletion mode, Ca^{2+} ions are depleted from the stimulating electrode by applying an ion-depletion current i_d of $\leq 1\,\mu A$ for $t_d = 0$–3 min across the Ca^{2+} ISM between two centre electrodes. The depletion current i_d is at least one order of magnitude lower than the electrical threshold value i_s required for electrical stimulation. **b**, After depleting the ions at a given current i_d between the centre electrodes at a distance of 200 μm for duration t_d, a stimulus current i_s is injected from the two outer stimulating electrodes into the centre electrode covered with a few-micrometre-thick (5–20 μm) Ca^{2+} ISM while i_d across the ISM is off.

$i_s = 2$ and 20 μA at a pulse width of $t_p = 300\,\mu s$ or 1 ms, and a pulse frequency of $f = 1$ Hz. Using a microfabricated Ca^{2+} ISM on the sciatic nerve of a frog, we achieved a decrease of the electrical threshold value from 7.4 μA to 4.4 μA (approximately 40% decrease) without applying any ion depletion current i_d before stimulation, as shown in Fig. 3. This reduction of threshold was achieved solely based on the stimulus current i_s, which triggered Ca^{2+} ion depletion and electrical stimulation simultaneously. To lower the threshold further, we first applied a depletion current of $i_d = 1\,\mu A$ across a Ca^{2+} ISM for $t_d = 1$ min and then applied a stimulation electrical pulse i_s directly thereafter. In this way, we could decrease the threshold to 2.2 μA. These measurements were repeated at least four times in different animal preparations, and we achieved an average reduction of the threshold by ~40% with direct ISM stimulation, and a further 20% with 1 min Ca^{2+} depletion before stimulation was achieved.

In Fig. 4a, we systematically investigate the influence of ion depletion time i_d on the threshold. As a control experiment to verify the effect of Ca^{2+} ion depletion on nerve excitability, we also used polyvinyl chloride (PVC) membranes without Ca^{2+}

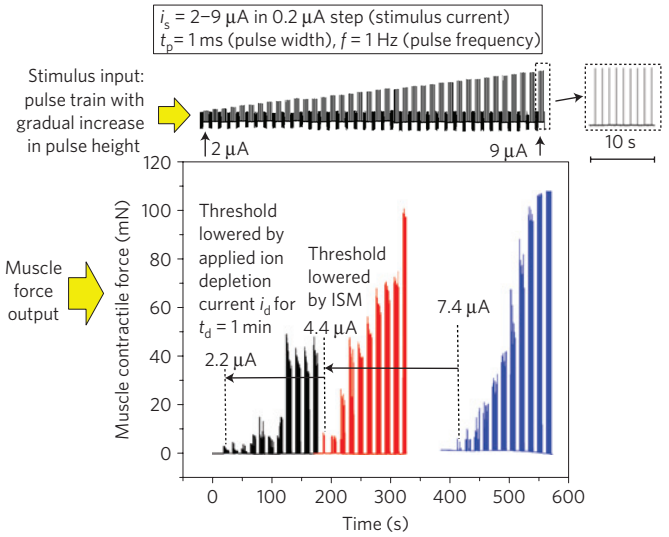

Figure 3 | Comparison of excitability without and with modulating Ca^{2+} ion concentration. The minimum electrical current required to elicit a muscle contraction was lowered from $i_s = 7.4\,\mu A$ (plot in blue) to 4.4 μA (plot in red) when directly stimulating with a Ca^{2+} ISM deposited on the cathode without any previous ion-depletion current (at $t_d = 0$). When applying ion-depletion current $i_d = 1\,\mu A$ for $t_d = 1$ min before stimulation, we could further reduce the threshold to 2.2 μA (plot in black).

ion-specific ionophore. As shown in Fig. 3, the Ca^{2+} ISM enabled a decrease in the threshold value directly without applying a further ion-depletion current ($t_d = 0$ min), simply by using the stimulus current flowing into the cathode for Ca^{2+} ion depletion. If a further ion-depletion current $i_d = 1\,\mu A$ is applied before stimulation for t_d = 1–3 min, we could observe a further decrease of the threshold value as a function of depletion time t_d. In a control experiment with the PVC membrane[8,9], there was no noticeable decrease of the threshold value when stimulating without ion-depletion current i_d applied before stimulation. When applying i_d, however, we could also observe a continuous decrease of the threshold as a function of ion-depletion time t_d. This result indicates that the subthreshold current i_d applied between the two centre electrodes also increased axonal excitability. However, the amount of net threshold reduction was ~10% higher in the case of the Ca^{2+} membrane from $t_d = 0$ to $t_d = 1$ min. It is evident from this result that there are two coupled effects influencing axonal excitability: (1) the effect of subthreshold d.c. current leading to electrotonus[10,11] and (2) the effect of Ca^{2+} ion depletion. A stimulation experiment with ISM in 10% donkey serum showed that our device could also work in a serum-rich environment such as body fluid.

When switching the polarity of the electrodes (ISM on the anode versus cathode), we also observed a decrease of the threshold, as shown in Fig. 4b. This result confirmed that the subthreshold current i_d contributes to a decrease of the threshold in addition to the Ca^{2+} ion concentration modulation. When we compared the final reduction ratios of both polarities, the ion-depletion mode with the ISM on the cathode was more effective by ~10% up to $t_d = 2$ min after offsetting the initial difference of the reduction ratios at $t_d = 0$ min (p value of 0.0133). As shown in Fig. 4c, the decrease in the threshold value was dependent on the ion-depletion current i_d. At $i_d = 100$ nA and 10 nA, no significant reduction of the threshold could be achieved when depleting longer than $t_d = 1$ min (p value of 0.0107). On the basis of these data, an estimation of energy expenditure for our electrochemical stimulation method is given in comparison with functional electrical stimulation in Supplementary Information.

The storing capacity of the ISM printed on the microfabricated electrode will be limited owing to its finite thickness (typically 5–20 μm). The duration of the depletion current as well as its amplitude will define the amount and speed of ion depletion from the nerve into the pores of the membrane. However, once the ion reservoir capacity of the membrane has been reached, it is likely that the effect of ion depletion on the electrical stimulus threshold will no longer be present owing to the steady state of ionic concentration, and eventually the ionic concentrations are restored to their normal level due to homeostasis. To 'empty' the ion reservoir, the polarity of the electrodes needs simply to be reversed. A potential solution to address this issue of limited ion storage capacity in the membrane is to design a stimulation device where ISM material is used as a 'filter' rather than for 'storage' of the particular ion (see Supplementary Fig. S1).

Our *in vitro* experimental results using a microfabricated planar ISM, as well as a conventional ISM in the form of a glass pipette tip (see details of the fabrication of ion-selective pipette tips in the Methods section and experimental results in Supplementary Figs S2–S5), demonstrate that the depletion of Ca^{2+} ions can reduce the electrical threshold value by approximately 40% without a constant perfusion and approximately 20% under a constant perfusion of Ringer's solution. With a microfabricated ISM, we demonstrated that a Ca^{2+} ISM layer printed with a thickness of 5–20 μm on a planar microelectrode can be used as a selective ion reservoir to deplete and store the target ion from a zone adjacent to the nerve by controlling the potential/current across the ISM. To the best of our knowledge, this is the first time that a local *in situ* control of ion concentration has been used to achieve higher excitable states for electrical stimulation. This significant reduction of the electrical threshold value could be achieved at a depletion current of $i_d \leq 1\,\mu A$ (usually less than 2 V applied across the ISM to maintain the ion-depletion current in the microfabricated electrodes). It is likely that we can increase the efficacy of this method (in terms of speed and threshold reduction) by using higher ion-depletion currents. Nonetheless, water is hydrolysed at electrode potentials over approximately 2 V, and above this voltage chlorine ions can be oxidized at the electrode surface, potentially producing toxic compounds and limiting application potential. To overcome this limitation, we can further decrease the gap size between the electrodes (currently 200 μm).

We confirmed the role of Ca^{2+} ions in nerve excitation in a separate control experiment where the nerve was completely immersed in a Ca^{2+}-ion-depleted Ringer's bath solution (see Supplementary Fig. S6). In this context, an important point to consider is whether the isotonic Ringer's solution used in our *in vitro* experiment is representative of extracellular fluid *in vivo*. Ringer's solution as an isotonic solution with a similar ionic composition to that of the extracellular fluid is widely used in the study of peripheral nerve excitability[12]. The fact that the perineurium acts as a diffusion barrier to proteins and small molecules[13–15] and thereby reduces the influence of proteins and molecules on nerve excitability also supports the use of Ringer's solution in our experiments. The only difference regarding the use of extracellular fluid versus Ringer's solution is that the presence of proteins and other molecules might have an impact on the lifetime of the ISMs due to non-specific binding. Furthermore, we demonstrate that the force amplitude generated at the downstream muscle can be more accurately controlled by the Ca^{2+} ion depletion. This result implies that controlling muscle contraction is possible with a higher degree of resolution and/or dynamic range than with traditional functional electrical stimulation methods. It is hypothesized that the graded response of downstream muscle contraction may be due to the local manner of perturbing Ca^{2+} ion concentration (modulating ion concentration on one side of a fibre).

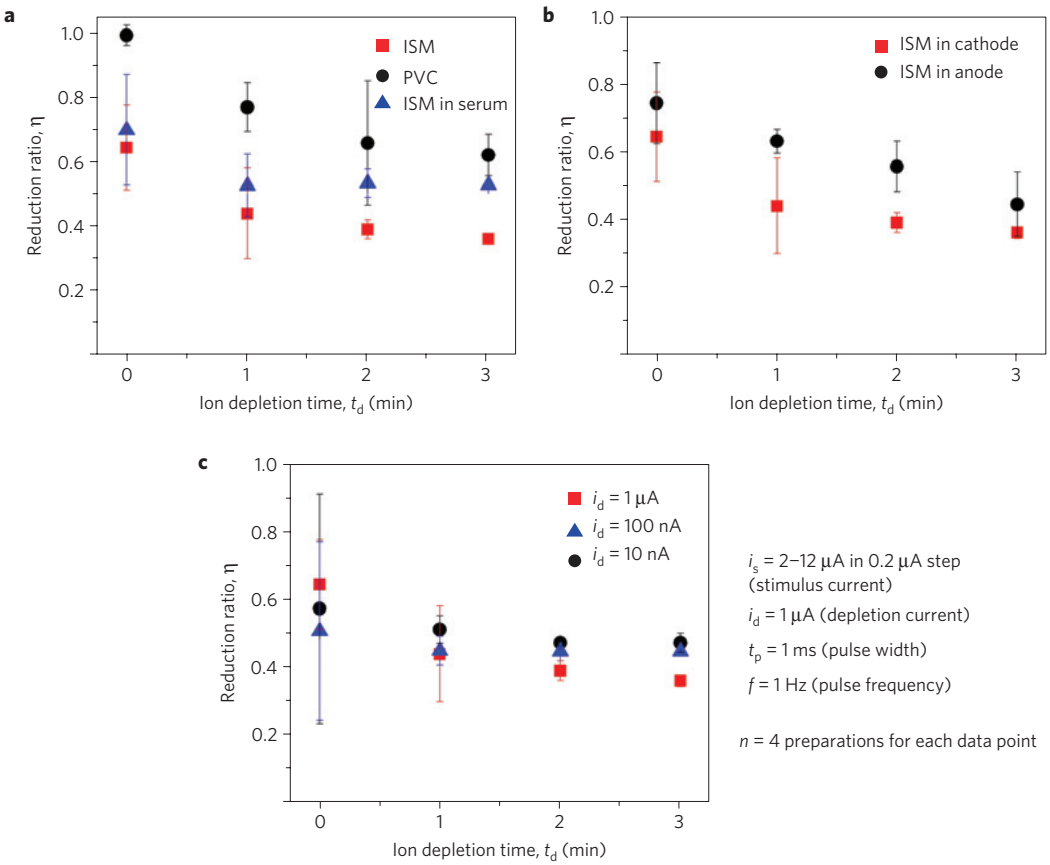

Figure 4 | Characterization of the electrochemical stimulation device under various parametric conditions. a, Comparison of the reduction ratios in Ringer's and serum environment. The reduction ratio is defined as $\eta =$ (threshold with ISM/threshold without ISM). The control experiment was carried out with a PVC membrane without Ca^{2+} ion-specific ionophore. For each data point, four different preparations were used. **b**, Influence of the polarity on the reduction ratio. It is evident that the reduction of the threshold was caused by two effects: subthreshold current i_d as well as Ca^{2+} ion depletion leading to higher axon excitability. **c**, Effect of the ion-depletion current i_d on the reduction ratio η. Increasing ion-depletion current i_d enhanced axonal excitability due to higher subthreshold current as well as higher ion depletion simultaneously.

Nerve conduction blocking with Ca^{2+} ISMs

Another important application of our ISM device is nerve conduction blocking. To investigate whether a modulation of the Ca^{2+} ion concentration along the nerve is an effective method of lowering the blocking threshold of the nerve signal conduction, we positioned an ISM device between the site of stimulation and the muscle in a bipolar, perpendicular configuration (Fig. 5). The anode was positioned closer to the proximal stimulating electrodes than the two cathodes. The direct current block of peripheral nerves has been previously demonstrated by several groups[16,17]. The Kilgore group reported a mean direct current of ~50 μA required to block the nerve signal in a frog sciatic nerve with spiral-shaped wires wrapped around the sciatic nerve at least five times[18]. Applying high-frequency a.c. has also been previously reported as one potential method for nerve conduction block[19]. This method enabled a rapidly reversible nerve conduction block in animal models[18]. In the frog, a sinusoidal or rectangular waveform (3–5 kHz and 0.5–2 mA_{p-p}) enabled the most consistent block[20]. However, no implant device has been demonstrated on the basis of this approach so far[19–21]. Compared with the electrodes without ISM (Fig. 5a), the planar microelectrodes with a surface-printed Ca^{2+} ISM enabled a 25–50% reduction of d.c. block threshold from $i_b = 50$–100 μA to 10–50 μA in 13 experiments (Fig. 5b). We could modulate the transmitted nerve signal by varying the d.c. block current applied. In addition, recovery to the previous twitch amplitude was almost instantaneous after turning off the d.c.

Nerve block caused by Na^+ and K^+ ion depletion

In addition to the Ca^{2+} ISM, we also tested a Na^+ ISM deposited on the cathode in the same device ('perpendicular geometry'). The hypothesis was that depleting extracellular Na^+ ions would lead to an action-potential block by eliminating the driving force behind action-potential generation, but we could not achieve any significant decrease of the blocking threshold. This finding may be due to the fact that extracellular Na^+ ion concentrations are generally high (requiring a much significantly higher perturbation current), and that Na^+ depleted regions may be too short to overcome the 'safety factor' of the nerve action-potential propagation. With a surface contact length of 10 mm between the membrane and the nerve for Na^+ ion depletion ('parallel geometry' in Supplementary Fig. S7a), we achieved a graded blocking of the sciatic nerve for an electrical stimulus by depleting the Na^+ ions from the nerve and its surroundings without continuous perfusion of Ringer's solution (Supplementary Fig. S7b). No muscle response was recorded even at higher electrical pulses with i_s over 30 μA after depleting Na^+ ions for 5 min with $i_d = 1$ μA across the Na^+ ISM when the twitch amplitude before the blocking was in the range of ~1 mN. At higher twitch amplitudes (~100 mN), however, a significantly larger ion depletion current was required between $i_d = 50$–100 μA to observe blocking after 5 min of Na^+ ion depletion. To investigate the reversibility of the signal blocking method by Na^+ ion depletion, we discontinued the ion-depletion current and immersed the nerve in Ringer's solution. Recovery to the original nerve excitability state required approximately 10 min

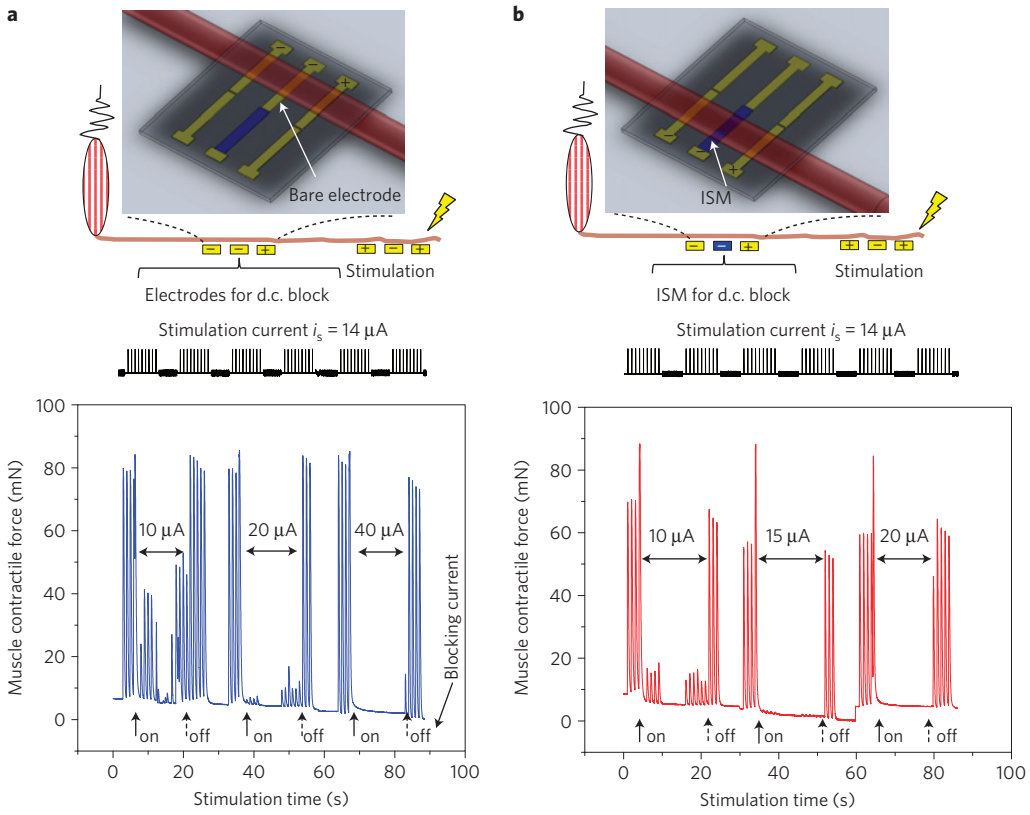

Figure 5 | Nerve-conduction-block experiment with a microfabricated ISM device. a, Schematic representation of the set-up for a study of the effect of ion concentration modulation on the d.c. nerve block. A single microfabricated ISM electrode array was positioned between the tripolar electrodes for electrical stimulation and the gastrocnemius muscle. First, the nerve was placed on top of the bare electrodes without ISM. The anode facing the stimulation site first was followed by two cathodes. At a d.c. block current of $i_b = 10\,\mu A$ we could achieve a partial blocking, and at a d.c. block current of $i_b = 40\,\mu A$ a total blocking. **b**, Application of nerve conduction block with a Ca^{2+} ISM on the cathode. When using the Ca^{2+} ISM, we could lower the d.c. block threshold to $i_b = 20\,\mu A$. The nerve regained its twitch amplitude almost immediately after turning off the d.c. block current.

in Ringer's solution. We also observed a similar blocking effect when modulating the K^+ ion concentration with a K^+ ion-selective pipette tip (see Supplementary Figs S8 and S9). It seemed that injecting K^+ ions from the pipette tip filled with 100 mM KCl solution onto the nerve was more effective in terms of nerve signal blocking than depleting these ions under continuous perfusion of Ringer's solution, which is expected because the incubation of a nerve in high K^+ concentration leads to elimination of the potassium concentration gradient across the membrane, and therefore the membrane potential.

Nerve blocking by Na^+ and K^+ depletion demonstrated limited reversibility. To restore the excitability of the nerve after blocking, incubation with Ringer's solution or a significant time delay were necessary, which is in contrast with the almost immediate reversibility of Ca^{2+}-ion-depletion-based blocking. The potassium ion concentration gradient across the membrane is the main determinant of the membrane resting potential. Therefore, significant modification of the K^+ concentration near the nerve could shift the resting potential, possibly inducing currents along the nerve. This concept may explain the 'difficulty' of re-gaining ion homeostasis. When using a cation-selective membrane such as Nafion with a reversed polarity of the ISM (the Nafion membrane deposited on the anodic side), which creates a general ion-depletion zone (depletes all ions), we also achieved a similar blocking effect (Supplementary Fig. S10). This nerve-blocking state could be reversed by immersing the nerve in a bath of Ringer's solution for 10 min (see Supplementary Fig. S11). We repeated this cycle of inhibition and relaxation three times with an immersion of the nerve in Ringer's solution for 10 min between each cycle. In addition to Nafion, we could potentially achieve a similar effect with other cation-selective membrane materials such as poly(3,4-ethylenedioxythiophene) doped with poly(styrene sulphonate), which, as an electrically conducting organic polymer, was previously used to demonstrate electronic control of the ion homeostasis in neurons[22].

One key constraint that could limit the effectiveness of our approach is the permeability of the perineurium for ions. The perineurium constitutes a diffusion barrier to electron-dense tracers[23,24] and to small ions[25–27]. Consequently, there is a lag in the change of nerve excitability as a result of the change of ion concentrations in the extracellular fluid[28]. Also, depending on the diameter of the nerve, the majority of axons could be insensitive to the local ionic manipulation. Our confocal imaging data showed that a change of ionic concentration due to the ISM was limited to ~120 μm inside the nerve fibre (see details of confocal imaging in the Methods section and results in Supplementary Fig. S12). To translate these ideas to various neural prosthetic devices, longer-term, *in vivo* reliability and safety studies need to be carried out. Electrochemical reduction/oxidation processes at the electrodes, as well as any pH changes at the ISMs, could be undesirable because they may alter the chemical composition of the extracellular fluid, producing cytotoxic compounds and effects[29]. The pH shift at a current density of $10\,\mu A\,mm^{-2}$ seems to be of lesser concern for our experiments because the Ringer's solution was adequately buffered[30]. In these ISMs, because the current density was significantly lower, $\leq 318\,nA\,mm^{-2}$ for the ion-selective pipette electrode and $\sim 5\,\mu A\,mm^{-2}$ for the planar ion-selective electrodes, we would expect fewer problems with pH shift. Regarding the nerve-blocking

effect, ISMs in combination with a.c.[21] could potentially lower the blocking threshold in a similar manner as the d.c.

In sum, we have demonstrated a means of using ISMs in modulating the activation and inhibition of nerve impulses in a reversible, graded fashion. These findings have potentially significant implications for the design of low-power, compact, neural prosthetic devices that selectively enhance nerve action potentials or inhibit unwanted motor endplate action potentials or noxious nerve stimulation. The devices demonstrated in this paper are readily applicable as electrochemical nerve manipulation technology, controlled entirely electrically without the need for chemical (ion) reservoirs and other complicated set-up. We visualize that these types of electrode can be fabricated on a flexible substrate[31] without any modification, for better enmeshing and contouring for nerve fibres and cells of various shapes and sizes. In this method, the ion-depletion time could be significantly reduced because of increased surface contact area between the nerve and electrodes. With a projected flexible electrode system wrapped around the nerve, it is expected that we could achieve an even greater control of nerve excitability. Further studies will be conducted to find out whether this electrochemical stimulation technique can be extended to mammalian nerves. Finally, given the broad roles of ions such as Ca^{2+} in cellular signalling, the use of ISMs demonstrated in this work could be used to directly control important ionic species near biological tissues and cells.

Methods

Fabrication of ion-selective planar microelectrodes. The planar microelectrodes were fabricated using the standard lift-off process. In brief, we patterned a 1-μm-thick positive photoresist spin-coated on a 1-mm-thick glass wafer photolithographically. After depositing 50 nm Ti and 200 nm Au layers on the patterned glass wafer using e-beam deposition, the photoresist layer was removed in acetone overnight. Before depositing an ISM, the electrode was dehydrated at 90 °C on a hotplate for 24 h and then silanized with *N*, *N*-dimethyltrimethylsilylamine (Fluka) for 60 min (ref. 32). To deposit/print an ISM on top of a planar microelectrode, we placed a polydimethylsiloxane microchip with a single microfluidic channel (300–1,500 μm wide and 50 μm deep) and sealed it against the planar electrode after an optical alignment using a stereomicroscope. The ISM for each specific ion was made using commercially available ion-selective cocktails from Sigma Aldrich, potassium ionophore I for K^+ ion, sodium ionophore I for Na^+ ion and ETH124 (calcium ionophore II) for Ca^{2+} ion, in a plasticized amorphous polymer matrix such as PVC. The ISM was composed according to methods published[8,9,32]. Using capillary force, the microchannel was filled with the ion-selective resin mixture (10–20 wt% for Ca^{2+} ionophore, 20 wt% for K^+ and Na^+ ionophores in a plasticized amorphous matrix consisting of 35.8 mg PVC in 0.4 ml cyclohexanone). The polydimethylsiloxane channel was immediately removed once the electrode has been covered with the ion-selective resin, and the electrodes were stored in a dark room and dried for 12 h under ambient conditions. To deposit cation-selective membrane on the planar electrodes, we used Nafion perfluorinated resin solution with 20 wt% of lower aliphatic alcohols and water (Sigma Aldrich).

Fabrication of ion-selective pipette tips. The ISM construct consisted of an ISM at the top of an electrolyte solution (either 100 mM $CaCl_2$ or 100 mM KCl depending on the ion species to modulate)-filled glass pipette or PVC tip, with one silver wire (127 μm OD) located inside and a second one outside the pipette tip. To enhance the adhesion of the ion-selective resin to the glass pipette surface, the pipettes were dehydrated at 90 °C on a hotplate for 24 h and then silanized with *N*, *N*-dimethyltrimethylsilylamine (Fluka) for 60 min (ref. 32). The ISM components were dissolved in 0.4 ml cyclohexanone (Fluka). The membrane resin was pipetted 2 mm into a glass pipette with an OD of 1.5 mm and ID of 0.8 mm (World Precision Instruments). The height of the resin inside the pipette was controlled to 2 mm and dried for 24 h under ambient conditions.

Frog preparation. North American bullfrogs (*Rana catesbeiana*) were purchased from Connecticut Valley Biological Supply Company. Their size was 5″–6″. Each frog acquired from Animal Facilities was sedated with 0.1–0.2 wt% MS222 (ethyl 3-aminobenzoate, methanesulphonic acid) for about 30 min or until the frog was no longer mobile. This protocol was approved by the Massachusetts Institute of Technology Committee on Animal Care. Preparation of nerves and gastrocnemius muscles is described in Supplementary Information.

Measurement of muscle contractile force and compound action potentials. The end of the gastrocnemius muscle was attached to a dual-range force transducer FT-302 (iWorx) with string. The force was recorded with a four-channel data recorder (iWorx 214) and analysed with LabScribe2 software. We used a standard Ringer's solution to keep the nerve and the muscle hydrated. In addition to the muscle contraction force, we also measured the compound action potential with a home-made amplifier and a PC-based oscilloscope. The ion depletion/injection current was applied with a dual-channel system SourceMeter 2612 from Keithley.

Confocal imaging. We used a Fluo-4 NW calcium-assay kit (F36206, Invitrogen) to measure the Ca^{2+} ion concentration change inside the sciatic nerve. We added 2.5 ml of assay buffer and 100 μl of probenecid to Fluo-4 NW dye mix to obtain 10 mM probenecid concentration. We immersed a 10-mm-long fresh sciatic nerve into Fluo-4 NW solution and maintained a 2 h immersion time to saturate the nerve with Fluo-4 dye. For confocal imaging, we used a Zeiss confocal microscope (LSM 710). To observe the sciatic nerve while depleting ions, we used a planar microelectrode composed of transparent indium–tin oxide deposited to a layer thickness of 100 nm by a sputtering process. The electrodes were 10 mm long and 750 μm wide. A sciatic nerve was positioned on top of the Ca^{2+} ISM for confocal imaging, as shown in Supplementary Fig. S12a. For measurement of the fluorescence intensity in the confocal microscope, we increased the *z* height by 6.17 μm from the bottom of the device into the sciatic nerve. More details of the experimental set-up and imaging data are given in Supplementary Information.

Received 14 December 2010; accepted 16 September 2011; published online 23 October 2011

References

1. Katz, B. *Society of Experimental Biology Symposia 4. Structural Aspects of Cell Physiology* 16–38 (Cambrige Univ. Press, 1952).
2. Hodgkin, A. L. & Huxley, A. F. A quantitative description of membrane current and its application to conduction and excitation in nerve. *J. Physiol.* **117,** 500–544 (1952).
3. Kandel, E. R., Schwartz, J. H. & Jessell, T. M. *Principles of Neural Science* (McGraw-Hill, 2000).
4. Brink, F. The role of calcium ions in neural processes. *Pharmacol. Rev.* **6,** 243–298 (1954).
5. Brink, F., Bronk, D. W. & Larrabee, M. G. Chemical excitation of nerve. *Ann. New York Acad. Sci.* **47,** 457–485 (1946).
6. Santini, J. T., Cima, M. J. & Langer, R. A controlled-release microchip. *Nature* **397,** 335–338 (1999).
7. Chen, J. & Wise, K. D. *Solid-State Sensor and Actuator Workshop* 256–259 (Cleveland Heights, 1994).
8. Ammann, D., Buehrer, T., Schefer, U., Mueller, M. & Simon, W. Intracellular neutral carrier-based Ca^{2+} microelectrode with subnanomolar detection limit. *Pfluegers Arch.* **409,** 223–228 (1987).
9. Baudet, S., Hove-Madsen, L. & Bers, D. M. in *Methods in Cell Biology* Vol. 40 (ed. Nuccitelli, R.) Ch. 4 (American Society for Cell Biology, Academic, 1994).
10. Bostock, H., Cikurel, K. & Burke, D. Threshold tracking techniques in the study of human peripheral nerve. *Muscle Nerve* **21,** 137–158 (1998).
11. Bostock, H. & Grafe, P. Acitivity-dependent excitability changes in normal and demyelinated rat spinal root axons. *J. Physiol.* **365,** 239–257 (1985).
12. Ask, P., Levitan, H., Robinson, P. J. & Rapoport, S. I. Peripheral nerve as an osmometer: Role of the perineurium in frog sciatic nerve. *Am. J. Physiol.* **244,** C75–C81 (1983).
13. Weerasuriya, A., Spangler, R. A., Rapoport, S. I. & Taylor, R. E. AC impedance of the perineurium of the frog sciatic nerve. *Biophys. J.* **46,** 167–174 (1984).
14. Bradbury, M. W. & Crowder, J. Compartments and barriers in the sciatic nerve of the rabbit. *Brain Res.* **103,** 515–526 (1976).
15. Abbott, N. J., Mitchell, G., Ward, K. J., Abdullah, F. & Smith, I. C. An electrophysiological method for measuring the potassium permeability of the nerve perineurium. *Brain Res.* **776,** 204–213 (1997).
16. Petruska, J. C., Hubscher, C. H. & Johnson, R. D. Anodally focused polarization of peripheral nerve allows discrimination of myelinated and unmyelinated fiber input to brainstem nuclei. *Exp. Brain Res.* **121,** 379–390 (1998).
17. Manfredi, M. Differential block of conduction of large fibers in peripheral nerve by direct current. *Arch. Ital. Biol.* **108,** 52–71 (1970).
18. Bhadra, N. & Kilgore, K. L. Direct current electrical conduction block of peripheral nerve. *IEEE Trans. Neural Syst. Rehabil. Eng.* **12,** 313–324 (2004).
19. Tanner, J. A. Reversible blocking of nerve conduction by alternating-current excitation. *Nature* **195,** 712–713 (1962).
20. Kilgore, K. L. & Bhadra, N. Nerve conduction block utilising high-frequency alternating current. *Med. Biol. Eng. Comput.* **42,** 394–406 (2004).
21. Bhadra, N. & Kilgore, K. L. High-frequency nerve conduction block. *Conf. Proc. IEEE Eng. Med. Biol. Soc.* **7,** 4729–4732 (2004).
22. Isaksson, J. *et al.* Electronic control of Ca^{2+} signalling in neuronal cells using an organic electronic ion pump. *Nature Mater.* **6,** 673–679 (2007).
23. Olsson, Y. & Reese, T. S. Permeability of vasa nervorum and perineurium in mouse sciatic nerve studied by fluorescence and electron microscopy. *J. Neuropathol. Exp. Neurol.* **30,** 105–119 (1971).

24. Waggener, J. D., Bunn, S. M. & Beggs, J. The diffusion of ferritin within the peripheral nerve sheath, an electron microscopy study. *J. Neuropathol. Exp. Neurol.* **24,** 430–443 (1965).
25. Feng, T. P. & Liu, Y. M. The connective tissue sheath of the nerve as effective diffusion barrier. *J. Cell. Physiol.* **34,** 1–16 (1949).
26. Krnjevic, K. The distribution of Na and K in cat nerves. *J. Physiol.* **128,** 473–488 (1955).
27. Seneviratne, K. N. & Weerasuriya, A. Nodal gap substance in diabetic nerve. *J. Neurol. Neurosurg. Psychiatry* **37,** 502–513 (1974).
28. Weerasuriya, A. Permeability of endoneurial capillaries to K, Na and Cl and its relation to peripheral nerve excitability. *Brain Res.* **419,** 188–196 (1987).
29. Prodanov, D., Marani, E. & Holsheimer, J. Functional eletric stimulation for sensory and motor functions: Progress and problems. *Biomed. Rev.* **14,** 23–50 (2003).
30. Mortimer, J. in *Handbook of Physiology—the Nervous System II* (eds Brookshart, J. M. & Mountcastle, V. B.) (American Physiology Society, 1981).
31. Kim, D. H. *et al.* Stretchable and foldable silicon integrated circuits. *Science* **320,** 507–511 (2008).
32. Guenat, O. T. *et al.* Microfabrication and characterization of an ion-selective microelectrode array platform. *Sens. Actuat. B* **105,** 65–73 (2005).

Acknowledgements

This work was conducted with support from a Massachusetts Institute of Technology faculty discretionary research fund, a Harvard Catalyst Grant from the Harvard Clinical and Translational Science Center (National Institutes of Health Award UL1 RR 025758) and financial contributions from Harvard University and its affiliated academic health-care centres.

Author contributions

Y-A.S. carried out fabrication of ion-selective electrodes and membranes, experimental work and confocal imaging. R.M., A.N.R., A.M.S.I., D.M. and A.T. conducted experimental work and data analysis. J.H. and S.J.L. carried out project planning. A.N.R., Y-A.S., S.J.L. and J.H. wrote the manuscript.

Additional information

The authors declare competing financial interests: details accompany the paper at www.nature.com/naturematerials. Supplementary information accompanies this paper on www.nature.com/naturematerials. Reprints and permissions information is available online at http://www.nature.com/reprints. Correspondence and requests for materials should be addressed to J.H. or S.J.L.